

---

# QUANTIFYING THE HIV RESERVOIR WITH DILUTION ASSAYS AND DEEP VIRAL SEQUENCING

---

A PREPRINT

 **Sarah C. Lotspeich<sup>†</sup>**

Department of Statistical Sciences  
Wake Forest University  
Winston-Salem, North Carolina, U.S.A.

 **Brian D. Richardson<sup>†</sup>**

Department of Biostatistics  
University of North Carolina at Chapel Hill  
Chapel Hill, North Carolina, U.S.A.

 **Pedro L. Baldoni**

The Walter and Eliza Hall Institute of Medical Research  
Parkville, Victoria, Australia

 **Kimberly P. Enders**

Department of Biostatistics  
University of North Carolina at Chapel Hill  
Chapel Hill, North Carolina, U.S.A.

 **Michael G. Hudgens**

Department of Biostatistics  
University of North Carolina at Chapel Hill  
Chapel Hill, North Carolina, U.S.A.  
mhudgens@email.unc.edu

1 February 2023

## ABSTRACT

People living with HIV on antiretroviral therapy often have undetectable virus levels by standard assays, but “latent” HIV still persists in viral reservoirs. Eliminating these reservoirs is the goal of HIV cure research. The quantitative viral outgrowth assay (QVOA) is commonly used to estimate the reservoir size, i.e., the infectious units per million (IUPM) of HIV-persistent resting CD4+ T cells. A new variation of the QVOA, the Ultra Deep Sequencing Assay of the outgrowth virus (UDSA), was recently developed that further quantifies the number of viral lineages within a subset of infected wells. Performing the UDSA on a subset of wells provides additional information that can improve IUPM estimation. This paper considers statistical inference about the IUPM from combined dilution assay (QVOA) and deep viral sequencing (UDSA) data, even when some deep sequencing data are missing. The proposed methods accommodate assays with wells sequenced at multiple dilution levels and include a novel bias-corrected estimator for small samples. The proposed methods are evaluated in a simulation study, applied to data from the University of North Carolina HIV Cure Center, and implemented in the open-source R package `SLDeepAssay`.

**Keywords** Distinct viral lineages · infectious units per million · maximum likelihood estimation · missing data · Poisson distribution · serial limiting dilution assay.

## 1 Introduction

Modern antiretroviral therapy (ART) is a highly effective treatment for people living with HIV, often helping them achieve viral suppression (i.e., have a level of virus in their blood that is below the limit of detection of standard assays) and eliminating their risk of transmission to others. However, despite viral suppression, “latent” HIV-infected cells, which do not produce viral proteins and are not recognized by the immune system, will remain. These latently infected

---

<sup>†</sup>These authors contributed equally to the work.

cells are commonly referred to as the HIV reservoir [Ndung'u et al., 2019]. If a person living with HIV stops taking ART, these latently infected cells will result in viral rebound, sometimes in a matter of weeks [Li et al., 2021]. Thus, the continued use of ART is necessary to maintain viral suppression, but there are costs and potential toxicities associated with lifelong use [Chawla et al., 2018]. Furthermore, as of 2021, only an estimated 75% of the 38.4 million people living with HIV worldwide currently have access to treatment [UNAIDS, 2022], and it is unclear whether a feasible path towards 100% treatment coverage exists. For these reasons, developing a cure for HIV that eliminates the latent viral reservoir and removes the need for ART is of high scientific and public health importance [Ndung'u et al., 2019].

In HIV cure studies, a primary endpoint is the concentration of latent HIV-infected cells, often measured in infectious units per million cells (IUPM). This concentration is not directly measurable and is typically estimated through a serial limiting dilution (SLD) assay, wherein wells with known dilution levels (i.e., known numbers of cells) are tested for the presence of at least one cell with infectious virus. Repeating this process over multiple replicate wells (i.e., wells with the same dilution level) and at various dilution levels provides information for estimating the IUPM in the source population of cells (i.e., the person taking ART).

The quantitative viral outgrowth assay (QVOA) is one standard SLD assay for quantifying the HIV reservoir, as measured by the IUPM of resting CD4+ T cells. The QVOA tests wells for the presence of the HIV p24 antigen, an indicator that at least one cell within the well is HIV-infected. Various statistical methods have been proposed for drawing inference about the IUPM based on data from dilution assays like the QVOA. Myers et al. [1994] proposed a maximum likelihood estimator (MLE) of the IUPM, along with a corresponding exact confidence interval derived by inverting the likelihood ratio test. Trumble et al. [2017] proposed a bias-corrected MLE (BC-MLE), adapted from Hepworth and Watson [2009], that corrects for upward bias of the MLE in small samples. The open-source `SLDAssay` software package implements the methods described above.

The Ultra Deep Sequencing Assay of the outgrowth virus (UDSA), a variation of the QVOA, is a newer SLD assay for measuring the latent HIV reservoir that tests for the presence of distinct viral lineages (DVLs) in each well. Whereas the QVOA tests only for the presence of HIV in a given well, the UDSA provides additional information about the number of DVLs therein. Assuming that most latently infected cells are infected with at most one DVL, knowing the number of DVLs provides an improved lower bound (relative to the QVOA) for the number of infected cells in that well. Often, the QVOA is initially performed to identify the wells that are infected with at least one DVL (i.e., are positive), and then the UDSA is performed on a subsample of positive wells; this leads to a missing data problem. Lee et al. [2017] proposed an MLE of the IUPM that incorporates partially observed additional information from the UDSA.

This paper justifies and extends existing methods to quantify the HIV reservoir from dilution assay and deep viral sequencing data. The Lee et al. [2017] estimator is shown to be consistent and asymptotically normal, and a bias-corrected MLE that accounts for the additional information from the UDSA is introduced. The possibility of the UDSA not detecting all DVLs in the source population is considered. Further, the MLE is extended to accommodate assays with multiple dilution levels, fully capturing all available information. The proposed methods are compared with existing methods via simulation studies and an application to real assay data from the University of North Carolina (UNC) HIV Cure Center. The rest of the paper proceeds as follows. In Section 2, notation is defined, assumptions are given, and the proposed methods are introduced. The simulation studies are presented in Section 3, and data from the UNC HIV Cure Center are analyzed in Section 4. The paper concludes with a discussion in Section 5.

## 2 Methods

For simplicity, Sections 2.1–2.5 assume that only assay data from a single dilution level are utilized. In Section 2.6, the methods are extended to the multiple dilution level setting.

### 2.1 Model and data

Assume that  $M$  replicate wells, each with the same number of cells, are sequenced via the QVOA, out of which  $M_P$  are found to be HIV-positive (i.e., to contain at least one DVL) and  $M_N$  are found to be HIV-negative. Assume for now that there are one million cells per well; Section 2.6 discusses the scenario with assay data from a single dilution level other than one million cells per well. Of the  $M_P$  positive wells, a subset of size  $m$  ( $m \leq M_P$ ) is deep-sequenced via the UDSA to obtain DVL information. Following Myers et al. [1994] Trumble et al. [2017], and Lee et al. [2017], assume:

- (A1) Cells are sampled randomly into the  $M$  wells from a larger source population.
- (A2) For each DVL, infected cells are randomly distributed amongst the wells.
- (A3) The QVOA and UDSA have perfect sensitivity and specificity.

Assay data are collected in two stages. *Stage 1 (QVOA)*: First, let  $X_j$  be a latent variable denoting the number of cells in well  $j$  that are infected with any DVL of HIV,  $j \in \{1, \dots, M\}$ . From the QVOA, indicator variables  $W_j = \mathbf{I}(X_j \geq 1)$  are observed in place of  $X_j$ , where  $W_j = 1$  if well  $j$  is positive and  $W_j = 0$  otherwise. *Stage 2 (UDSA)*: Denote by  $n$  the number of DVLs detected across the deep-sequenced wells,  $n \in \{0, 1, 2, \dots\}$ . Then, let  $X_{ij}$  be a latent variable denoting the number of cells in well  $j$  that are infected with observed DVL  $i$  of HIV,  $i \in \{1, \dots, n\}$ . In practice, the indicator variables  $Z_{ij} = \mathbf{I}(X_{ij} \geq 1)$  are observed directly from the UDSA instead of the  $X_{ij}$ . For a given well  $j$ , let the vector  $\mathbf{Z}_j = (Z_{1j}, \dots, Z_{nj})^T$  contain indicators of whether each of the  $n$  DVLs was detected therein. The random variables from Stages 1 and 2 are related via  $W_j = \mathbf{I}(\sum_{i=1}^n Z_{ij} \geq 1)$ .

Let the vector  $\mathbf{X}_i = (X_{i1}, \dots, X_{iM})^T$  contain the numbers of cells infected with DVL  $i$  in wells 1 through  $M$ . Suppose that the components  $X_{ij}$  are independent (A2) and Poisson distributed with rate  $\lambda_i \geq 0$ , where the DVL-specific rate parameter  $\lambda_i$  represents the mean number of cells per well infected with DVL  $i$ . The counts of infected cells should be approximately Poisson distributed when the number of cells per well is large and  $\lambda_i$  is small [Myers et al., 1994, Trumble et al., 2017]. Because so few cells are latently infected and, of those that are, most are infected by only one DVL, the indicators for each DVL (i.e.,  $Z_{1j}, \dots, Z_{nj}$ ) are approximately independent. Then, the indicators  $W_j$  and  $Z_{ij}$  follow Bernoulli distributions with  $\Pr(W_j = 1) = 1 - \exp(-\sum_{i=1}^n \lambda_i)$  and  $\Pr(Z_{ij} = 1) = 1 - \exp(-\lambda_i)$ . Because it is assumed that there are one million cells per well,  $\sum_{i=1}^n \lambda_i$  is the IUPM, which will be denoted by  $\Lambda$ .

Often, not all of the  $M_P$  positive wells are sequenced with the UDSA, which introduces missingness. Let  $R_j$  be a complete data indicator for well  $j$ , defined such that  $R_j = 1$  if the well has complete data and  $R_j = 0$  otherwise. Complete data are available from the  $m$  positive wells with the additional UDSA information and from the  $M_N$  negative wells. (No data are missing from the negative wells because, under (A3), negative QVOA results imply that there are zero DVLs in the negative wells.) Thus, the number of wells with complete data is  $\sum_{j=1}^M R_j = m + M_N$ .

## 2.2 Likelihood construction

All wells are initially tested for the presence of infectious virus using the QVOA, so the Stage 1 variables  $\mathbf{W} = (W_1, \dots, W_M)^T$  are fully observed. However, since only a subset of the positive wells undergoes the UDSA in Stage 2,  $\mathbf{Z} = (\mathbf{Z}_1, \dots, \mathbf{Z}_M)$  will have missing data for the  $(M_P - m)$  unsequenced positive wells. Based on this data collection scheme, illustrated in Figure 1, there are three types of well-level observations to consider:

- (T1) A negative well ( $R_j = 1, W_j = 0, \mathbf{Z}_j = \mathbf{0}$ );
- (T2) A positive well that was deep sequenced ( $R_j = 1, W_j = 1, \mathbf{Z}_j = \mathbf{z}_j$ ); and
- (T3) A positive well that was not deep sequenced ( $R_j = 0, W_j = 1, \mathbf{Z}_j = ?$ ).

For the two positive well types, at least one element in the  $\mathbf{Z}_j$  vector equals one since the well has to be positive for at least one DVL.

To incorporate all available information on all wells, the observed-data likelihood function is proportional to

$$L(\boldsymbol{\lambda} | \mathbf{W}, \mathbf{Z}, \mathbf{R}) = \prod_{j=1}^M \Pr_{\boldsymbol{\lambda}}(W_j, \mathbf{Z}_j)^{R_j} \Pr_{\boldsymbol{\lambda}}(W_j)^{(1-R_j)},$$

where  $\Pr_{\boldsymbol{\lambda}}(W_j, \mathbf{Z}_j)$  is the joint probability mass function (PMF) of  $(W_j, \mathbf{Z}_j)$  and  $\Pr_{\boldsymbol{\lambda}}(W_j)$  is the marginal PMF of  $W_j$ . Because wells are selected for deep sequencing based only on the fully observed QVOA results  $\mathbf{W}$ , the UDSA results  $\mathbf{Z}$  are missing at random (MAR) for the unsequenced wells [Little and Rubin, 2002]. Therefore, the distribution of  $\mathbf{R}$  can be omitted from the likelihood for  $\boldsymbol{\lambda}$ . Under the assumption of perfect QVOA sensitivity and specificity (A3), and since  $W_j$  is completely determined by  $\mathbf{Z}_j$ ,  $\Pr_{\boldsymbol{\lambda}}(W_j | \mathbf{Z}_j) = 1$  and it follows that  $\Pr_{\boldsymbol{\lambda}}(W_j, \mathbf{Z}_j) = \Pr_{\boldsymbol{\lambda}}(W_j | \mathbf{Z}_j) \Pr_{\boldsymbol{\lambda}}(\mathbf{Z}_j) = \Pr_{\boldsymbol{\lambda}}(\mathbf{Z}_j)$ . Assuming independence between the DVLs,  $\Pr_{\boldsymbol{\lambda}}(\mathbf{Z}_j) = \prod_{i=1}^n \Pr_{\lambda_i}(Z_{ij})$ . Thus,

$$L(\boldsymbol{\lambda} | \mathbf{W}, \mathbf{Z}, \mathbf{R}) = \prod_{j=1}^M \left[ \prod_{i=1}^n \{1 - \exp(-\lambda_i)\}^{Z_{ij}} \exp(-\lambda_i)^{(1-Z_{ij})} \right]^{R_j} \{1 - \exp(-\Lambda)\}^{(1-R_j)},$$

which simplifies to

$$\left[ \prod_{i=1}^n \{1 - \exp(-\lambda_i)\}^{\sum_{j=1}^M Z_{ij} R_j} \exp(-\lambda_i)^{\sum_{j=1}^M (1-Z_{ij}) R_j} \right] \{1 - \exp(-\Lambda)\}^{\sum_{j=1}^M (1-R_j)}.$$

		negative wells				positive wells								
		1	2	...	$M_N$	1	2	3	...	$m$	1	2	...	$M_p - m$
QVOA Result		-	-	...	-	+	+	+	...	+	+	+	...	+
DVL 1		0	0	...	0	1	0	1	...	0	?	?	...	?
DVL 2		0	0	...	0	1	1	0	...	1	?	?	...	?
DVL 3		0	0	...	0	0	1	0	...	1	?	?	...	?
DVL 4		0	0	...	0	0	1	1	...	1	?	?	...	?
DVL 5		0	0	...	0	1	1	0	...	0	?	?	...	?
⋮		⋮	⋮	⋮	⋮	⋮	⋮	⋮	⋮	⋮	⋮	⋮	⋮	⋮
DVL n		0	0	...	0	1	0	1	...	1	?	?	...	?

Figure 1: Illustration of the data collection scheme from the QVOA and UDSA at a single dilution level

For ease of notation, let  $Y_i = \sum_{j=1}^M Z_{ij} R_j$  and  $\mathbf{Y} = (Y_1, \dots, Y_n)^T$ . It follows from the two-stage data collection procedure (Section 2.1) that  $\sum_{j=1}^M (1 - Z_{ij}) R_j = (M_N + m) - Y_i$  and  $\sum_{j=1}^M (1 - R_j) = M - (M_N + m)$ . Therefore,  $(M_N, \mathbf{Y})$  are sufficient statistics for  $\lambda$  and the likelihood can be rewritten as

$$L(\lambda | M_N, \mathbf{Y}) = \left[ \prod_{i=1}^n \{1 - \exp(-\lambda_i)\}^{Y_i} \exp(-\lambda_i)^{M_N + m - Y_i} \right] \{1 - \exp(-\Lambda)\}^{M - (M_N + m)}. \quad (1)$$

### 2.3 Maximum likelihood estimation

The MLE of the DVL-specific rate parameters, denoted  $\hat{\lambda} = (\hat{\lambda}_1, \dots, \hat{\lambda}_n)^T$ , is found by maximizing the observed-data log-likelihood  $\ln\{L(\lambda | M_N, \mathbf{Y})\}$  based on (1) with respect to  $\lambda$ , under the constraint that Poisson rates must be non-negative. When a subset of the positive wells are sequenced, the MLE  $\hat{\lambda}$  does not appear to have a closed-form solution but can be obtained numerically. However, analytical solutions do exist in two special cases: (i) when no positive wells are deep-sequenced or (ii) when all positive wells are deep-sequenced. See Web Appendix A for details on finding the MLE.

Assuming that the UDSA data are indeed MAR and under suitable regularity conditions, the MLE  $\hat{\lambda}$  will be consistent for the true values  $\lambda$  and asymptotically normally distributed [Little and Rubin, 2002]. That is,  $\sqrt{M}(\hat{\lambda} - \lambda) \rightsquigarrow \mathcal{N}_n(\mathbf{0}, \Sigma)$ , where  $\rightsquigarrow$  denotes convergence in distribution and  $\mathcal{N}_n(\mathbf{0}, \Sigma)$  is an  $n$ -variate normal distribution with mean vector  $\mathbf{0}$  and covariance matrix  $\Sigma$ . By the invariance property of MLEs, it follows that the MLE for the IUPM  $\Lambda = \sum_{i=1}^n \lambda_i$  is  $\hat{\Lambda} = \sum_{i=1}^n \hat{\lambda}_i$ . Moreover, by the continuous mapping theorem and the delta method,  $\hat{\Lambda}$  is a consistent and asymptotically normal estimator of  $\Lambda$ .

The asymptotic covariance matrix of  $\hat{\lambda}$  is given by the inverse of the Fisher information matrix, i.e.,  $\Sigma = \mathcal{I}(\lambda)^{-1} = E\left\{-\partial^2 l(\lambda | M_N, \mathbf{Y}) / \partial \lambda \partial \lambda^T\right\}^{-1}$ , which can be consistently estimated by  $\hat{\Sigma} = \mathcal{I}(\lambda)^{-1}|_{\lambda=\hat{\lambda}}$ . A derivation of  $\hat{\Sigma}$  is given in Web Appendix B. Further, the standard error of the IUPM estimator  $\hat{\Lambda}$  can be estimated by  $\widehat{SE}(\hat{\Lambda}) = (\sum_{i=1}^n \sum_{j=1}^M \hat{\Sigma}_{i,j})^{1/2}$ , where  $\hat{\Sigma}_{i,j}$  denotes the  $(i, j)$ th element of  $\hat{\Sigma}$ . By the delta method, a  $100(1 - \alpha)\%$  Wald confidence interval for the log IUPM  $\ln(\Lambda)$  has endpoints  $\ln(\hat{\Lambda}) \pm z_{\alpha/2} \widehat{SE}(\hat{\Lambda}) / \hat{\Lambda}$ , where  $z_{\alpha/2}$  denotes the  $(1 - \alpha/2)$ th percentile of the standard normal distribution. Exponentiating these endpoints gives a strictly positive confidence interval for  $\Lambda$ .

## 2.4 Bias correction for small samples

In SLD assay settings, the MLE will be upwardly biased with a small number of replicate wells, such that  $\hat{\lambda}$  tends to overestimate the size of a person's latent HIV reservoir [Trumble et al., 2017]. A bias-corrected MLE (BC-MLE) based on Hepworth and Watson [2009] was proposed by Trumble et al. [2017]. The Trumble et al. [2017] bias correction is intended for a one-dimensional parameter estimator and therefore cannot be applied to  $\hat{\lambda}$ . Instead, a bias-correction method for the multi-dimensional setting, developed by Hashemi and Schneider [2021], is adapted here. The method involves subtracting a correction term from the MLE  $\hat{\lambda}$  to reduce the order of the bias from  $\mathcal{O}(M^{-1})$  to  $\mathcal{O}(M^{-2})$ .

Following Hashemi and Schneider [2021], the bias of the MLE  $\hat{\lambda}$  can be expressed as

$$E(\hat{\lambda} - \lambda) = \Sigma \mathbf{A}(\lambda) \text{vec}(\Sigma) + \mathcal{O}(M^{-2}), \quad (2)$$

where  $\mathbf{A}(\lambda) = [\mathbf{A}_1(\lambda), \dots, \mathbf{A}_n(\lambda)]$  is the  $n \times n^2$  matrix with  $n \times n$  submatrices

$$\mathbf{A}_i(\lambda) = \frac{\partial}{\partial \lambda_i} \mathcal{I}(\lambda) - \frac{1}{2} E \left\{ \frac{\partial^3}{\partial \lambda \partial \lambda^T \partial \lambda_i} l(\lambda | M_N, \mathbf{Y}) \right\}$$

and  $\text{vec}(\Sigma)$  denotes the  $n^2 \times 1$  column vector obtained by stacking the columns of  $\Sigma$ . The components of submatrix  $\mathbf{A}_i(\lambda)$  are derived in Web Appendix C. Equation (2) motivates the BC-MLE for the DVL-specific rate parameters:  $\hat{\lambda}^* = (\hat{\lambda}_1^*, \dots, \hat{\lambda}_n^*)^T = \hat{\lambda} - B(\hat{\lambda})$ , where  $B(\hat{\lambda}) = \hat{\Sigma} \mathbf{A}(\hat{\lambda}) \text{vec}(\hat{\Sigma})$ . Finally, the BC-MLE for the IUPM is  $\hat{\Lambda}^* = \sum_{i=1}^n \hat{\lambda}_i^*$ . Conveniently, the MLE and the BC-MLE have the same asymptotic distribution. To see this, note that the bias correction term  $B(\hat{\lambda}) = \mathcal{O}_p(M^{-1})$ , i.e.,  $MB(\hat{\lambda})$  is bounded in probability, so  $\sqrt{M}B(\hat{\lambda})$  converges in probability to zero. Then, using Slutsky's theorem,

$$\sqrt{M}(\hat{\lambda}^* - \lambda) = \sqrt{M} \left[ \{\hat{\lambda} - B(\hat{\lambda})\} - \lambda \right] = \left\{ \sqrt{M}(\hat{\lambda} - \lambda) - \sqrt{M}B(\hat{\lambda}) \right\} \rightsquigarrow \mathcal{N}_n(\mathbf{0}, \Sigma),$$

i.e.,  $\hat{\lambda}^*$  is also a consistent and asymptotically normal estimator of  $\lambda$ . Moreover, the asymptotic covariance of  $\hat{\lambda}^*$  can be consistently estimated by  $\hat{\Sigma}$ . However, by construction,  $\hat{\lambda}^*$  will tend to have smaller bias than  $\hat{\lambda}$  for a small number of wells.

## 2.5 Estimation with undetected viral lineages

When a person living with HIV is tested with the UDSA, only a very small subset of their CD4+ T cells are obtained (typically by leukapheresis). The person may have additional DVLs in their population of CD4+ T cells that were not present in the subset of cells sampled, in which case the UDSA would not detect these additional DVLs, even with perfect sensitivity and specificity. Below it is shown that the proposed IUPM estimator can still be viewed as an MLE, even in the presence of undetected viral lineages.

Suppose that there are  $n'$  DVLs present in an individual living with HIV,  $n$  of which are detected by the UDSA,  $n' \in \{n+1, n+2, n+3, \dots\}$ . This leaves  $n' - n$  undetected viral lineages, with corresponding counts of infected cells  $\mathbf{Y}' = (Y_{n+1}, \dots, Y_{n'})^T$  that are independent and Poisson distributed with rates  $\lambda_{i'}$ ,  $i' \in \{n+1, \dots, n'\}$ . With some abuse of notation, let  $Y_0 = Y_{n+1} + \dots + Y_{n'}$  denote the number of wells infected with any of the undetected DVLs. Then,  $Y_0$  also has a Poisson distribution with rate  $\lambda_0 = \lambda_{n+1} + \dots + \lambda_{n'}$ , and, since no wells are infected with these lineages,  $Y_0 = 0$  is observed. Thus, the augmented likelihood function accounting for all DVLs (detected and undetected) can be written as

$$\begin{aligned} L'(\lambda' | M_N, \mathbf{Y}, Y_0) \\ = \left[ \prod_{i=0}^n \{1 - \exp(-\lambda_i)\}^{Y_i} \exp(-\lambda_i)^{(M_N + m - Y_i)} \right] \left\{ 1 - \exp \left( - \sum_{i=0}^n \lambda_i \right) \right\}^{(M - M_N - m)}, \end{aligned} \quad (3)$$

where  $\lambda' = (\lambda_0, \lambda^T)^T$ . Given that DVLs  $n+1, \dots, n'$  are undetected, a reasonable heuristic estimate for the rate of their sum  $\lambda_0$  is zero. In fact, it is proven in the Appendix that the MLE for  $\lambda_0$  is zero. That is, the vector  $\hat{\lambda}'$  that maximizes (3) necessarily satisfies  $\hat{\lambda}_0 = 0$ . When estimating  $\Lambda$ , this implies that using the sum of the  $n$ -dimensional MLE  $\hat{\lambda}$  from the original likelihood in (1) is equivalent to using the sum of the  $(n+1)$ -dimensional MLE  $\hat{\lambda}'$  from the augmented likelihood in (3). In other words, summing the DVL-specific MLEs for the detected DVLs gives the MLE for the sum of *all the* DVL-specific rate parameters, detected or not.

## 2.6 Incorporating multiple dilution levels

So far, it has been assumed that the assay was conducted at a single dilution level, with each replicate well containing one million ( $10^6$ ) cells. In practice, dilution levels other than one million cells per well may be used. Moreover, multiple dilution levels are often tested with the QVOA to pinpoint one or more appropriate dilution levels for the UDSA (i.e., dilution levels with sufficient positive wells). The methods from Sections 2.1–2.5 are now adapted to handle these two cases.

First, consider the setting where an assay is done at a single dilution level, but each replicate well contains  $u \times 10^6$  cells for some  $u > 0$ . Continue to let  $\lambda_i$  be the mean count of cells per well infected with DVL  $i$ ,  $i \in \{1, \dots, n\}$ . Now, let  $\tau_i$  be the mean count of cells *per million* infected with DVL  $i$ , and denote by  $\boldsymbol{\tau} = (\tau_1, \dots, \tau_n)^T$  the vector of DVL-specific IUPMs for all  $n$  DVLs. If  $u = 1$ , as assumed in previous sections, then  $\boldsymbol{\lambda} = \boldsymbol{\tau}$  and  $\Lambda = T$ . More generally, for a dilution level of  $u$ , the DVL-specific IUPMs and mean counts per cell are related through  $\boldsymbol{\tau} = \boldsymbol{\lambda}/u$ . Using this relationship, the likelihood in (1) can be rewritten as a function of  $\boldsymbol{\tau}$  by substituting  $\boldsymbol{\lambda} = u\boldsymbol{\tau}$  and defining  $\tilde{L}(\boldsymbol{\tau}|M_N, \mathbf{Y}, u) = L(u\boldsymbol{\tau}|M_N, \mathbf{Y})$ . Then, the MLE for  $\boldsymbol{\tau}$  is the value  $\hat{\boldsymbol{\tau}}$  that maximizes the likelihood  $\tilde{L}$  over the parameter space  $[0, \infty)^n$ , and, from it, the IUPM is estimated as  $\hat{T} = \sum_{i=1}^n \hat{\tau}_i$ .

Now, consider the second case where assay data  $(M_N^{(d)}, \mathbf{Y}^{(d)}, u^{(d)})$ ,  $d \in \{1, \dots, D\}$ , are available from replicate wells at  $D$  distinct dilution levels,  $D \in \{1, 2, \dots\}$ . Let  $M_N^{(d)}$ ,  $\mathbf{Y}^{(d)}$ , and  $u^{(d)}$  denote the number of negative wells, vector of UDSA results, and dilution level, respectively, for the  $d$ th dilution. Assume independence between replicate wells and across dilution levels; this is the natural extension of assumption (A1) to the multiple dilution level setting. Then, the joint likelihood given data from all  $D$  dilution levels is equal to the product of the individual likelihoods given data from each dilution level:

$$\tilde{L}(\boldsymbol{\tau}|M_N, \mathbf{Y}, \mathbf{u}) = \prod_{d=1}^D \tilde{L}(\boldsymbol{\tau}|M_N^{(d)}, \mathbf{Y}^{(d)}, u^{(d)}), \quad (4)$$

where  $\mathbf{M}_N = (M_N^{(1)}, \dots, M_N^{(D)})^T$ ,  $\mathbf{Y} = (\mathbf{Y}^{(1)}, \dots, \mathbf{Y}^{(D)})$ , and  $\mathbf{u} = (u^{(1)}, \dots, u^{(D)})^T$ . The MLE for the vector of DVL-specific IUPMs is the value  $\hat{\boldsymbol{\tau}}$  that maximizes the likelihood (4), and the corresponding IUPM can be calculated as their sum.

The MLE  $\hat{T}$  from this joint likelihood (4) is once again consistent for the true IUPM  $T$  and asymptotically normal with asymptotic variance  $\sum_{i=1}^n \sum_{j=1}^n \tilde{\Sigma}_{ij}$ , where  $\tilde{\Sigma} = \tilde{L}(\boldsymbol{\tau})^{-1} = E[-\partial^2 \ln \{\tilde{L}(\boldsymbol{\tau}|M_N, \mathbf{Y}, \mathbf{u})\} / \partial \boldsymbol{\tau} \partial \boldsymbol{\tau}^T]^{-1}$ . The same bias correction method introduced in Section 2.4 can be applied to the multiple dilution level setting. Details on estimating  $\tilde{\Sigma}$  and computing the bias correction term in this setting are given in Web Appendix D. Note that the likelihood from Myers et al. [1994], which uses QVOA data only, is a special case of the likelihood in (4) where none of the positive wells are deep sequenced (i.e.,  $m = 0$ ). Thus, (4) can be used even when deep sequencing is not done; see special case (ii) in Web Appendix A.

## 3 Simulation

Simulation studies were performed to assess the proposed methods. Various settings were considered, inspired by real-world dilution assay studies with a single (Section 3.1) or multiple (Section 3.2) dilution levels. In addition to demonstrating the methods' validity, these simulations illustrate the notable efficiency gains from incorporating deep viral sequencing.

### 3.1 Simulations with a single dilution level

Data for a single dilution assay were simulated as follows. First, full results from the UDSA were generated as the DVL-specific infection indicators  $Z_{ij}$  for all wells,  $j \in \{1, \dots, M\}$ , and DVLs,  $i \in \{1, \dots, n'\}$ , from independent Bernoulli distributions with  $\Pr(Z_{ij} = 1) = 1 - \exp(-\lambda_i)$ . Results from the QVOA were then calculated as  $W_j = I(\sum_{i=1}^n Z_{ij} \geq 1)$  for all wells. The number of wells to undergo the UDSA was computed as  $m = \lfloor qM_P \rfloor$ , where  $q$  was the fixed proportion of positive wells that undergo the UDSA and  $\lfloor \cdot \rfloor$  denotes the nearest integer function. Based on  $q$ , a random sample of  $M_P - m$  positive wells were set to be missing their  $Z_{ij}$  information for all DVLs.

The simulation studies utilized a fully factorial design by considering all possible combinations of:  $M = 12, 14$ , or  $32$  replicate wells;  $n' = 6, 12$ , or  $18$  DVLs; proportions  $q = 1, 0.75$ , or  $0.5$  of positive wells that underwent the UDSA; and IUPM  $T = 0.05$  or  $1$ . These choices of parameters, which were motivated by the real data used in Section 4, led to  $54$  unique simulation settings defined by  $(M, n', q, T)$ . For simplicity, the single dilution level was chosen to be  $u = 1$ .

million cells per well, so  $T = \Lambda$ . In addition, two allocations of the IUPM  $T$  across the  $n'$  DVLs were considered: (i) *constant rate*, i.e., the same IUPM for all DVLs such that  $\tau_i = T/n'$  for  $i \in \{1, \dots, n'\}$ , and (ii) *non-constant rate*, i.e., a larger IUPM for the last  $n'/2$  DVLs such that  $\tau_i = T/(2n')$  for  $i \in \{1, \dots, n'/2\}$  versus  $\tau_i = 3T/(2n')$  for  $i \in \{n'/2 + 1, \dots, n'\}$ . Both allocations were applied for  $T = 1$ ; for  $T = 0.5$  only the constant rate scenario was considered. Two extreme results were possible: (i) all wells were negative, in which case the UDSA would not be done, or (ii) all wells were positive and a particular DVL was detected in each deep sequenced well, in which case the IUPM estimators would be infinite. While (i) never happened, (ii) occurred in 98 out of 81,000 simulations (0.1%); in these cases the simulated assay data were discarded and resimulated.

Four IUPM estimators were applied to each simulated assay: (i) MLE without UDSA, (ii) BC-MLE without UDSA, (iii) MLE with UDSA, and (iv) BC-MLE with UDSA. All estimators have been implemented in R packages, with (i) and (ii) in *SLDAssay* [Trumble et al., 2017] and (iii) and (iv) in *SLDeepAssay* (newly developed to accompany this paper). Estimators (ii) and (iv) were expected to have smaller bias than (i) and (iii) in small samples, and estimators (iii) and (iv) were expected to be more precise than (i) and (ii) due to the added DVL information from the UDSA.

A number of metrics are reported for comparison of the four IUPM estimators, summarizing the 1000 data sets simulated for each setting. The relative bias (“bias”) was computed by dividing (i) the mean differences between the estimated and true IUPM across replications by (ii) the true IUPM. The average standard error (ASE) and empirical standard error (ESE) were computed as the empirical mean of the standard error estimator and the empirical standard deviation of the IUPM estimators, respectively. Finally, the empirical coverage probability (CP) for the 95% confidence interval was computed as the proportion of simulations where the true IUPM fell between the lower and upper bounds of the interval.

Detailed results for a single dilution assay with IUPM of  $T = 1$  and a constant rate of infected cells for all DVLs can be found in Table 1. As expected, the two BC-MLEs had very little bias in all settings (both  $\leq 3\%$ ). Meanwhile, the uncorrected MLEs saw bias as large as 10%; this bias improved, though, as either (i) the number of wells  $M$  increased or (ii) the proportion  $q$  being deep sequenced increased (for the estimators with UDSA). Bias for all estimators was unchanged by an increasing number of DVLs  $n'$ .

Overall, the standard error estimators approximated the empirical standard errors well. For the MLE without UDSA, the ASE overestimated the ESE, but this was resolved as  $M$  increased. Based on ASE or ESE, the variability of the estimators with UDSA decreased when there were more replicate wells (i.e., larger  $M$ ) and, as expected, when the deep sequencing information was available for more wells (i.e., larger  $q$ ). In fact, the MLE and BC-MLE with UDSA were as much as 46% and 35% more efficient, respectively, than their counterparts without sequencing data. Despite needing to estimate more parameters when there were more DVLs, the variability of these estimators was stable as  $n'$  increased. The confidence intervals for the BC-MLEs were sometimes conservative with the smallest number of  $M = 12$  wells, but appeared reasonable for all other settings. Also, the over-coverage was slightly less severe for the estimators with UDSA than without. Otherwise, the confidence intervals achieved the appropriate coverage.

Results with a non-constant rate of infected cells were nearly identical (Web Table S1). Aside from uniformly smaller standard errors, results with the smaller a IUPM of  $T = 0.5$  were comparable to those discussed already (Web Table S2).

### 3.2 Simulations with multiple dilution levels

Data for an assay at multiple dilution levels were simulated as in Section 3.1, with a few modifications. For each scenario, three single dilution assay datasets were simulated, one for each of the  $D = 3$  dilution levels, and then combined for analysis. The following parameters were held fixed: (i) the true IUPM  $T = 1$ , (ii) the three dilution levels  $\mathbf{u} = (u_1, u_2, u_3) = (0.5, 1, 2)$  million cells per well, and (iii) the proportions of positive wells to be deep sequenced at the three dilution levels  $\mathbf{q} = (q_1, q_2, q_3) = (0, 0.5, 1)$ . The simulation settings varied by the number of replicate wells per dilution level,  $\mathbf{M} = (M_1, M_2, M_3) = (6, 12, 18), (9, 18, 27)$ , or  $(12, 24, 36)$ , and the number of DVLs,  $n' = 6, 12$ , or 18. Again, the IUPM could be allocated across the  $n'$  DVLs in a constant or non-constant way. No simulated data sets were discarded due to all wells being negative or positive (at all dilution levels). The same four estimators (MLE and BC-MLE, with and without UDSA) were applied to each simulated assay and compared with respect to bias, ASE, ESE, and CP.

Detailed results for the multiple dilution level assays with a constant rate of infected cells can be found in Table 2. In comparison to the single dilution simulations, the two uncorrected MLEs had relatively small bias ( $\leq 4\%$  versus  $\leq 10\%$ ). This is likely due to the fact that these estimators incorporate more information from the multiple dilutions. Still, the two bias-corrected MLEs further reduced this bias to  $\leq 1\%$  in all settings. The estimated standard errors were approximately consistent with the empirical ones, and the confidence intervals achieved near-nominal coverage, with empirical estimates between 94% and 97%. Across all settings, the estimators that used the UDSA had greater efficiency than those that did not, as reflected by the reductions in the ASE and ESE. As in the single dilution case, results with a non-constant rate of infected cells for the DVLs were nearly identical (Web Table S3).

Table 1: Simulation results with a single dilution level, assuming a constant rate of infected cells for all distinct viral lineages. The true IUPM in all settings was  $T = 1$ .

$n'$	$M$	$q$	Without UDSA								With UDSA							
			MLE				BC-MLE				MLE				BC-MLE			
			Bias	ASE	ESE	CP	Bias	ASE	ESE	CP	Bias	ASE	ESE	CP	Bias	ASE	ESE	CP
6	12	0.50	0.10	0.45	0.39	0.96	0.00	0.37	0.39	1.00	0.09	0.38	0.36	0.95	-0.02	0.34	0.36	0.98
		0.75	0.09	0.45	0.39	0.96	-0.01	0.37	0.39	0.99	0.06	0.34	0.33	0.94	-0.01	0.32	0.33	0.97
		1.00	0.09	0.46	0.39	0.95	-0.01	0.37	0.39	0.99	0.05	0.32	0.31	0.94	0.00	0.30	0.31	0.96
	24	0.50	0.04	0.31	0.27	0.96	-0.01	0.28	0.27	0.94	0.03	0.25	0.24	0.94	-0.01	0.24	0.24	0.96
		0.75	0.04	0.29	0.27	0.95	0.00	0.27	0.27	0.94	0.03	0.23	0.23	0.94	0.00	0.22	0.23	0.96
		1.00	0.04	0.29	0.27	0.96	0.00	0.27	0.27	0.95	0.02	0.21	0.22	0.95	-0.01	0.21	0.22	0.96
	32	0.50	0.03	0.24	0.23	0.97	0.00	0.22	0.23	0.97	0.02	0.20	0.21	0.96	-0.01	0.20	0.21	0.97
		0.75	0.03	0.24	0.23	0.95	0.00	0.23	0.23	0.95	0.02	0.20	0.20	0.95	0.00	0.19	0.20	0.96
		1.00	0.04	0.25	0.23	0.96	0.01	0.24	0.23	0.96	0.02	0.18	0.19	0.96	0.00	0.18	0.19	0.96
12	12	0.50	0.09	0.45	0.39	0.95	0.00	0.37	0.39	0.99	0.10	0.38	0.36	0.93	-0.01	0.35	0.36	0.97
		0.75	0.07	0.44	0.39	0.95	-0.02	0.37	0.39	0.98	0.04	0.33	0.32	0.94	-0.02	0.31	0.32	0.96
		1.00	0.10	0.44	0.39	0.96	0.00	0.36	0.39	0.99	0.07	0.31	0.31	0.94	0.02	0.30	0.31	0.96
	24	0.50	0.06	0.32	0.27	0.95	0.02	0.29	0.27	0.93	0.06	0.26	0.24	0.92	0.01	0.25	0.24	0.94
		0.75	0.04	0.29	0.27	0.96	0.00	0.27	0.27	0.94	0.03	0.22	0.22	0.95	-0.01	0.21	0.22	0.96
		1.00	0.02	0.29	0.27	0.96	-0.01	0.27	0.27	0.95	0.02	0.22	0.21	0.95	0.00	0.21	0.21	0.96
	32	0.50	0.03	0.24	0.23	0.97	0.00	0.23	0.23	0.97	0.04	0.20	0.21	0.95	0.00	0.20	0.21	0.96
		0.75	0.02	0.24	0.23	0.96	-0.01	0.23	0.23	0.96	0.02	0.19	0.19	0.94	0.00	0.19	0.19	0.95
		1.00	0.02	0.25	0.23	0.95	0.00	0.24	0.23	0.95	0.01	0.19	0.18	0.94	-0.01	0.18	0.18	0.95
	18	0.50	0.09	0.42	0.39	0.97	-0.01	0.35	0.39	1.00	0.09	0.36	0.35	0.95	-0.01	0.33	0.35	0.98
		0.75	0.06	0.42	0.39	0.96	-0.03	0.35	0.39	0.98	0.05	0.32	0.32	0.94	-0.01	0.31	0.32	0.96
		1.00	0.08	0.43	0.39	0.97	-0.02	0.36	0.39	0.99	0.05	0.31	0.30	0.95	0.00	0.29	0.30	0.96
	24	0.50	0.03	0.28	0.27	0.97	-0.01	0.26	0.27	0.95	0.03	0.24	0.24	0.94	-0.01	0.23	0.24	0.96
		0.75	0.04	0.30	0.27	0.96	-0.01	0.28	0.27	0.94	0.03	0.23	0.22	0.95	0.00	0.22	0.22	0.96
		1.00	0.03	0.30	0.27	0.96	-0.01	0.27	0.27	0.94	0.03	0.22	0.21	0.94	0.00	0.22	0.21	0.95
	32	0.50	0.03	0.26	0.23	0.95	0.00	0.25	0.23	0.95	0.03	0.21	0.21	0.95	0.00	0.20	0.21	0.96
		0.75	0.02	0.24	0.23	0.97	-0.01	0.23	0.23	0.97	0.02	0.19	0.19	0.95	0.00	0.19	0.19	0.96
		1.00	0.03	0.25	0.23	0.96	0.00	0.24	0.23	0.96	0.02	0.18	0.18	0.95	0.01	0.18	0.18	0.96

*Note:* **Bias** and **ESE** are, respectively, the empirical relative bias and standard error of the IUPM estimator; **ASE** is the average of the standard error estimator; **CP** is the empirical coverage probability of the 95% confidence interval for the IUPM. There were a total of 41 simulated assays out of 27,000 (0.2%) where the MLE and BC-MLE without UDSA were infinite that were excluded; all other entries are based on 1000 replicates.

Table 2: Simulation results with multiple dilution levels, assuming a constant rate of infected cells for all distinct viral lineages. In all settings, the true IUPM was  $T = 1$  and the proportions of positive wells that were deep sequenced at the three dilution levels were  $q = (0, 0.5, 1)$ .

$n'$	$M$	Without UDSA								With UDSA							
		MLE				Bias-Corrected MLE				MLE				Bias-Corrected MLE			
		Bias	ASE	ESE	CP	Bias	ASE	ESE	CP	Bias	ASE	ESE	CP	Bias	ASE	ESE	CP
6	(6, 12, 18)	0.04	0.20	0.23	0.95	0.00	0.20	0.21	0.95	0.02	0.14	0.15	0.94	0.00	0.14	0.15	0.95
		0.03	0.20	0.22	0.96	-0.01	0.20	0.20	0.97	0.02	0.14	0.14	0.95	0.00	0.14	0.14	0.96
		0.02	0.19	0.20	0.95	-0.01	0.19	0.19	0.95	0.01	0.13	0.14	0.94	0.00	0.13	0.13	0.95
	(9, 18, 27)	0.03	0.20	0.22	0.96	0.00	0.17	0.17	0.96	0.01	0.12	0.12	0.96	0.00	0.12	0.12	0.96
		0.02	0.17	0.17	0.96	0.00	0.17	0.17	0.96	0.01	0.12	0.12	0.96	0.00	0.12	0.12	0.96
		0.02	0.17	0.18	0.95	0.00	0.17	0.18	0.95	0.01	0.12	0.12	0.94	0.00	0.12	0.12	0.95
	(12, 24, 36)	0.02	0.19	0.20	0.95	-0.01	0.19	0.19	0.95	0.01	0.13	0.14	0.94	0.00	0.13	0.13	0.95
		0.02	0.17	0.17	0.96	0.00	0.17	0.17	0.96	0.01	0.13	0.14	0.94	0.00	0.13	0.13	0.95
		0.02	0.17	0.18	0.95	0.00	0.17	0.18	0.95	0.01	0.12	0.12	0.94	0.00	0.12	0.12	0.95
12	(6, 12, 18)	0.03	0.19	0.21	0.96	0.00	0.19	0.20	0.96	0.01	0.13	0.14	0.95	0.00	0.13	0.13	0.96
		0.02	0.17	0.17	0.96	0.00	0.17	0.17	0.96	0.01	0.12	0.12	0.96	0.00	0.12	0.12	0.96
		0.02	0.17	0.18	0.95	0.00	0.17	0.18	0.95	0.01	0.12	0.12	0.94	0.00	0.12	0.12	0.95
	(9, 18, 27)	0.02	0.17	0.17	0.96	0.00	0.17	0.17	0.96	0.01	0.12	0.12	0.96	0.00	0.12	0.12	0.96
		0.02	0.17	0.18	0.95	0.00	0.17	0.18	0.95	0.01	0.12	0.12	0.94	0.00	0.12	0.12	0.95
		0.02	0.17	0.18	0.95	0.00	0.17	0.18	0.95	0.01	0.12	0.12	0.94	0.00	0.12	0.12	0.95
	(12, 24, 36)	0.02	0.17	0.17	0.96	0.00	0.17	0.17	0.96	0.01	0.12	0.12	0.94	0.00	0.12	0.12	0.95
		0.02	0.17	0.18	0.95	0.00	0.17	0.18	0.95	0.01	0.12	0.12	0.94	0.00	0.12	0.12	0.95
		0.02	0.17	0.18	0.95	0.00	0.17	0.18	0.95	0.01	0.12	0.12	0.94	0.00	0.12	0.12	0.95
18	(6, 12, 18)	0.03	0.20	0.22	0.96	0.00	0.20	0.21	0.96	0.02	0.14	0.14	0.95	0.00	0.14	0.14	0.96
		0.04	0.20	0.23	0.94	0.00	0.20	0.21	0.95	0.02	0.14	0.14	0.95	0.00	0.14	0.14	0.96
		0.03	0.19	0.22	0.95	0.00	0.19	0.20	0.95	0.01	0.13	0.14	0.95	0.00	0.13	0.13	0.96
	(9, 18, 27)	0.03	0.20	0.23	0.94	0.00	0.20	0.21	0.95	0.02	0.14	0.14	0.95	0.00	0.14	0.14	0.96
		0.03	0.19	0.22	0.95	0.00	0.19	0.20	0.95	0.01	0.13	0.14	0.95	0.00	0.13	0.13	0.96
		0.03	0.19	0.22	0.95	0.00	0.19	0.20	0.95	0.01	0.13	0.14	0.95	0.00	0.13	0.13	0.96

*Note:* **Bias** and **ESE** are, respectively, the empirical relative bias and standard error of the IUPM estimator; **ASE** is the average of the standard error estimator; **CP** is the empirical coverage probability of the 95% confidence interval for the IUPM. All entries are based on 1000 replicates.

## 4 HIV Application

The proposed methods were used to analyze data for 17 people living with HIV on ART with suppressed viral load from the University of North Carolina HIV Cure Center. With multiple dilution QVOA and single dilution UDSA information, these data provide an additional opportunity to quantify the efficiency gain attributable to adding deep sequencing data over QVOA alone. For each subject (i.e., source population), an SLD assay was performed over  $D = 3\text{--}4$  dilution levels and with  $M = 6\text{--}36$  replicate wells per dilution level. For each subject, deep sequencing was done on 50–100% of positive wells at one dilution level (i.e.,  $0.5 \leq q \leq 1$ ). Details summarizing the assay results are provided in Web Table S4, and the full data are accessible as described in the data availability statement.

Methods applied to the UNC data included the estimators for multiple dilution QVOA with/without UDSA from Section 2.6 and those for single dilution QVOA with UDSA. Previously, Lee et al. [2017] compared the multiple dilution QVOA without UDSA to the single dilution QVOA with UDSA. However, this comparison does not isolate the benefits of using the multiple over single dilution QVOA or the addition of deep sequencing information, since the estimators used either multiple dilutions *or* deep sequencing, but not both. Here, comparisons are made between estimators based on (i) multiple dilution QVOA with versus without UDSA and (ii) single dilution UDSA with single versus multiple dilution QVOA.

Estimated log IUPM and 95% confidence intervals for the 17 people are provided in Figure 2. The log IUPM and its untransformed confidence interval were used to compare the methods' precision. More detailed analysis results for the IUPM can be found in Web Table S5. As expected, all subjects' bias-corrected IUPM estimates were smaller than their uncorrected ones; these smaller estimates are expected to be closer to the subjects' true HIV concentrations.

First, comparing the confidence intervals based on the multiple dilution QVOA with versus without UDSA highlights the precision gain attributable to incorporating the additional sequencing data. For some people, the confidence intervals using the UDSA data were remarkably narrower than those using the QVOA data alone. Incorporating the UDSA data led to the greatest increase in precision for Subject C12, who had 65 observed DVLs across 32 deep sequenced wells and a 57% narrower confidence interval (for the BC-MLE) when incorporating the UDSA. Meanwhile, for other people with fewer DVLs observed (e.g., Subject C13, who had seven observed DVLs from four sequenced wells), the confidence interval widths did not decrease when using sequencing information. Heuristically, the UDSA is more informative when more DVLs are detected and when more wells are deep sequenced.

Second, comparing the confidence intervals based on the UDSA with single versus multiple dilution QVOA illustrates the precision gain due to using data from all dilution levels. Again, large gains were seen for some subjects, while the inclusion of multiple dilutions did not change the precision much for others. Consider Subject C17, who had QVOA data available from four dilution levels. For this subject, using data from all dilution levels provided a 25% narrower confidence interval (for the BC-MLE) than only using data from the one deep sequenced dilution level. On the other hand, consider Subject C1, who had data from three dilution levels and had zero positive wells at the two unsequenced ones. For this person, the two unsequenced, all-negative dilution levels added little information. As a result, the confidence intervals for Subject C1 using UDSA and single or multiple dilution QVOA data are nearly identical. In general, the unsequenced dilutions were more informative when there were many more positive wells.

In summary, the estimators based on the multiple dilutions QVOA with UDSA make use of all available information and tend to have better precision than the estimators that ignore the other dilution levels or the UDSA data. The extent of the precision gain depends on the particular assay results.

## 5 Discussion

In this paper, methods were developed to analyze data from SLD assays augmented with additional information provided by deep sequencing. The estimator proposed by Lee et al. [2017], which uses information from dilution assays and deep sequencing, was given a formal justification and shown to be consistent and asymptotically normal. A bias-corrected MLE was proposed, and it was shown that the MLE is unchanged by the possibility of undetected viral lineages. The Lee et al. [2017] method was extended to the case where the QVOA and deep sequencing data were collected at multiple dilution levels. Simulations for both the single and multiple dilution settings demonstrated that the BC-MLE has low bias and its corresponding confidence interval achieves nominal coverage. The reduced bias and efficiency gains of the proposed methods relative to existing ones were demonstrated in an application to data from the UNC HIV Cure Center.

There are many directions for future work to expand inference procedures for combined dilution and deep sequencing assays. For the setting with only QVOA data, Myers et al. [1994] derived an exact confidence interval for the IUPM by inverting the likelihood ratio test. Myers et al. [1994] and Trumble et al. [2017] also proposed a goodness-of-fit

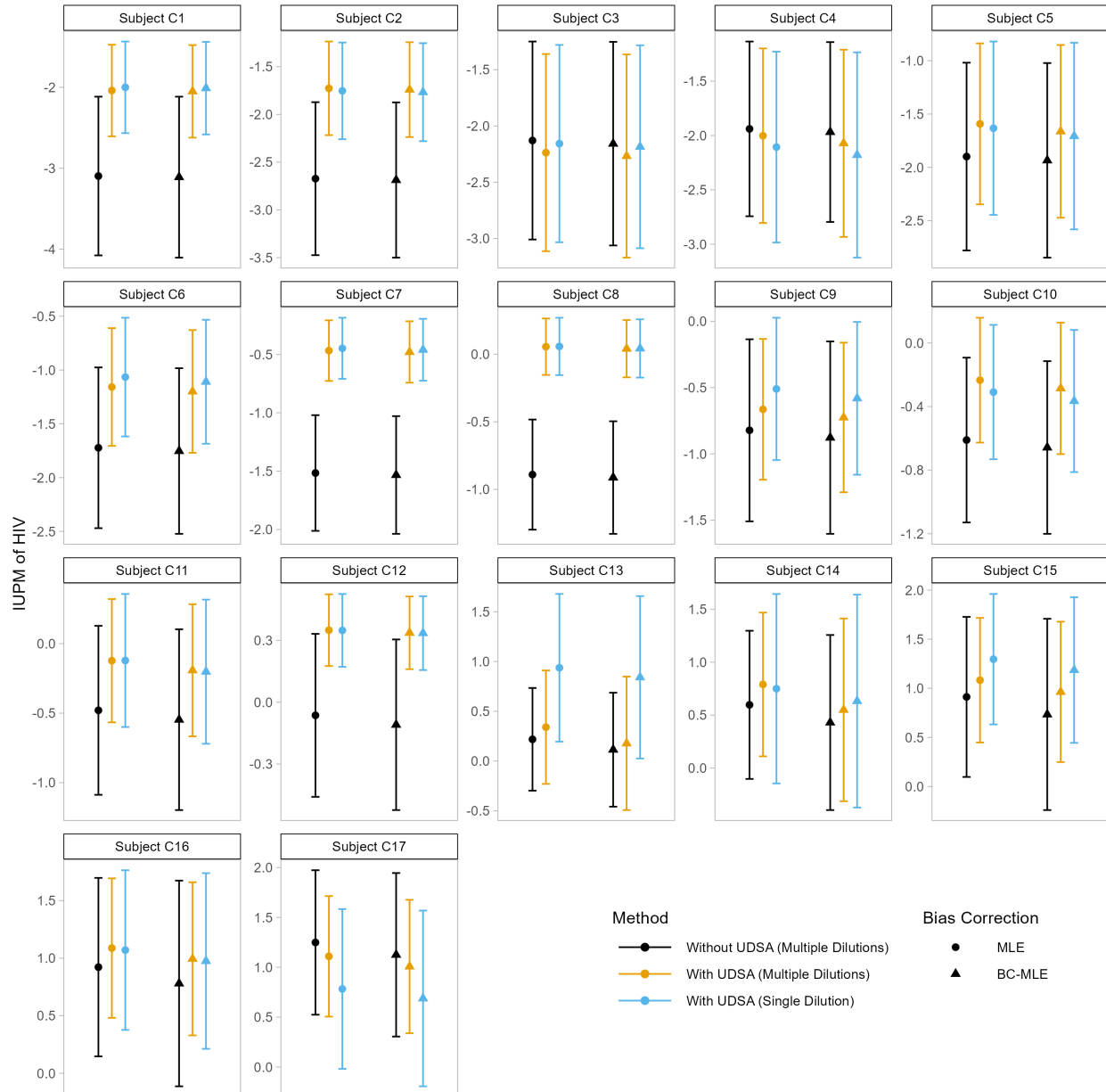


Figure 2: Estimated infectious units per million (IUPM) with 95% confidence intervals for 17 people living with HIV in the University of North Carolina HIV Cure Center Study. The IUPM and confidence interval were log transformed for comparisons of precision.

p-value (PGOF), which can be helpful in identifying possible technical problems with an assay. Calculating both the exact confidence interval and PGOF involve enumerating all possible assay outcomes. Without UDSA data, an assay with  $D$  dilution levels and  $M_d$  replicate wells per dilution level  $d$  has  $\prod_{d=1}^D (M_d + 1)$  possible outcomes. With UDSA data, the number of possible assay outcomes grows much more quickly. For example, if all positive wells were deep sequenced (i.e.,  $q_d = 1$  for  $d \in \{1, \dots, D\}$ ), and  $n$  DVLS were detected, then there are  $\prod_{d=1}^D (M_d + 1)^n$  possible outcomes. This combinatorial explosion makes calculating an exact confidence interval and PGOF for UDSA data computationally challenging. Therefore, developing a computationally feasible exact confidence interval and PGOF to this setting would be interesting areas for future research. Other extensions of the methods considered in this paper include (i) comparing IUPMs between a pair of samples taken from an individual before and after a treatment [Li et al., 2022] and (ii) comparing the distributions of IUPMs between two treatment groups with multiple individuals per group.

## Acknowledgements

This research was supported by the University of North Carolina at Chapel Hill Center for AIDS Research (CFAR), a National Institutes of Health (NIH) funded program P30AI50410, and NIH grant R37AI029168. The content is solely the responsibility of the authors and does not necessarily represent the official views of the NIH.

## Supporting Information

Web Appendices and Tables referenced in Sections 2–4, along with the R code for Sections 3–4, can be found on figshare at <https://figshare.com/projects/SLDeepAssay/155489>. The R package SLDeepAssay is available on GitHub at <https://github.com/sarahlotspeich/SLDeepAssay/>.

## Data Availability Statement

The data that support the findings of this study are openly available in figshare at <https://doi.org/10.6084/m9.figshare.21821229.v1>.

## References

T. Ndung'u, J. M. McCune, and S. G. Deeks. Why and where an hiv cure is needed and how it might be achieved. *Nature*, 576:397–405, 2019.

J. Z. Li, E. Aga, R. J. Bosch, M. Pilkinton, E. Kroon, L. MacLaren, M. Keefer, L. Fox, L. Barr, E. Acosta, J. Ananworanich, R. Coombs, J. W. Mellors, A. L. Landay, B. Macatangay, S. Deeks, R. T. Gandhi, D. M. Smith, and AIDS Clinical Trials Group A5345 Study Team. Time to viral rebound after interruption of modern antiretroviral therapies. *Clinical Infectious Diseases*, 74(5):865–870, 06 2021. ISSN 1058-4838. doi:10.1093/cid/ciab541. URL <https://doi.org/10.1093/cid/ciab541>.

A. Chawla, C. Wang, C. Patton, M. Murray, Y. Punekar, A. de Ruiter, and C. Steinhart. A review of long-term toxicity of antiretroviral treatment regimens and implications for an aging population. *Infectious Diseases and Therapy*, 7(2): 183–195, 2018.

UNAIDS. Global HIV & AIDS statistics — Fact sheet, 2022. URL <https://www.unaids.org/en/resources/fact-sheet>.

L. E. Myers, L. J. McQuay, and F. B. Hollinger. Dilution assay statistics. *Journal of Clinical Microbiology*, 450:10–16, 1994.

I. M. Trumble, A. G. Allmon, N. M. Archin, J. Rigdon, O. Francis, P. L Baldoni, and M. G. Hudgens. SLDAssay: A software package and web tool for analyzing limiting dilution assays. *Journal of Immunological Methods*, 32: 732–739, 2017.

G. Hepworth and R. Watson. Debiased estimation of proportions in group testing. *Applied Statistics*, 58:105–121, 2009.

S. Lee, S. Zhou, P. L. Baldoni, E. Spielvogel, N. M. Archin, M. G. Hudgens, D. M. Margolis, and R. Swanson. Quantification of latent HIV-1 reservoir using ultra deep sequencing and primer ID in a viral outgrowth assay. *Journal of Acquired Immune Deficiency Syndromes*, 74:221–228, 2017.

R. Little and D. Rubin. *Statistical Analyses with Missing Data*. New Jersey: John Wiley & Sons, Inc, 2002.

M. Hashemi and K. A. Schneider. Bias-corrected maximum-likelihood estimation of multiplicity of infection and lineage frequencies. *PLoS ONE*, 16(12):e0261889, 2021.

X. Li, S. May, I. M. Trumble, N. M. Archin, and M. G. Hudgens. Paired serial limiting dilution assays. *Statistics in Medicine*, 41:4809–4821, 2022.

## Appendix: Maximum Likelihood Estimation with Undetected Viral Lineages

In Section 2.5, an augmented likelihood function  $L'(\boldsymbol{\lambda}|M_N, \mathbf{Y}, Y_0)$  was given that accounts for the  $n' - n$  undetected viral lineages. Here, it is proven that the MLE for the mean count of infected cells  $\lambda_0$  for the undetected DVLs is necessarily zero.

*Proof.* Let  $\tilde{\boldsymbol{\lambda}} = (\tilde{\lambda}_0, \dots, \tilde{\lambda}_n)^T$  be an estimate of  $\boldsymbol{\lambda}$  where  $\tilde{\lambda}_0 > 0$ . To show that  $\tilde{\boldsymbol{\lambda}}$  cannot be the MLE for  $\boldsymbol{\lambda}$ , a distinct estimate  $\check{\boldsymbol{\lambda}}$  will be constructed such that  $L'(\check{\boldsymbol{\lambda}}|\mathbf{Y}, M_N) > L'(\tilde{\boldsymbol{\lambda}}|\mathbf{Y}, M_N)$ . This will prove that any estimate  $\tilde{\boldsymbol{\lambda}}$  where  $\tilde{\lambda}_0 > 0$  cannot be the MLE, or, equivalently, that the MLE for  $\lambda_0$  *must* be zero.

To construct such an estimate, choose an arbitrary DVL  $k$  from those detected by the UDSA,  $k \in \{1, \dots, n\}$ . Now, shift some mass  $\epsilon \in (0, \tilde{\lambda}_0)$  from the estimated parameter for the undetected viral lineages to the  $k$ th parameter, i.e., let

$$\check{\lambda}_0 = \tilde{\lambda}_0 - \epsilon \text{ and } \check{\lambda}_k = \tilde{\lambda}_k + \epsilon. \quad (5)$$

For all other DVLs (i.e.,  $i \in \{1, \dots, n\}$  and  $i \neq k$ ), leave the new estimates unchanged by defining  $\check{\lambda}_i = \tilde{\lambda}_i$ . By construction,  $\check{\boldsymbol{\lambda}}$  is distinct from  $\tilde{\boldsymbol{\lambda}}$  and satisfies  $\sum_{i=0}^n \check{\lambda}_i = \sum_{i=0}^n \tilde{\lambda}_i$ .

Now, consider the ratio of the augmented likelihood function (3) evaluated at  $\check{\boldsymbol{\lambda}}$  and  $\tilde{\boldsymbol{\lambda}}$ . Many terms cancel out, simplifying this likelihood ratio to

$$\frac{L(\check{\boldsymbol{\lambda}}|\mathbf{Y}, M_N)}{L(\tilde{\boldsymbol{\lambda}}|\mathbf{Y}, M_N)} = \frac{\left\{1 - \exp(-\check{\lambda}_k)\right\}^{Y_k} \exp(-\check{\lambda}_k)^{(M_N+m-Y_k)} \exp(-\check{\lambda}_{n+1})^{(M_N+m)}}{\left\{1 - \exp(-\tilde{\lambda}_k)\right\}^{Y_k} \exp(-\tilde{\lambda}_k)^{(M_N+m-Y_k)} \exp(-\tilde{\lambda}_{n+1})^{(M_N+m)}}.$$

To show that this likelihood ratio is greater than one, and thus that  $\tilde{\boldsymbol{\lambda}}$  cannot be the MLE since it does not maximize the augmented likelihood, recall that  $\check{\boldsymbol{\lambda}}$  was constructed from  $\tilde{\boldsymbol{\lambda}}$ . Therefore, using the definitions in (5), the likelihood ratio can be rewritten in terms of only  $\tilde{\boldsymbol{\lambda}}$  as

$$\frac{\left[1 - \exp\left\{-\left(\tilde{\lambda}_k + \epsilon\right)\right\}\right]^{Y_k} \exp\left\{-\left(\tilde{\lambda}_k + \epsilon\right)\right\}^{(M_N+m-Y_k)} \exp\left\{-\left(\tilde{\lambda}_{n+1} - \epsilon\right)\right\}^{(M_N+m)}}{\left\{1 - \exp(-\tilde{\lambda}_k)\right\}^{Y_k} \exp(-\tilde{\lambda}_k)^{(M_N+m-Y_k)} \exp(-\tilde{\lambda}_0)^{(M_N+m)}}$$

and further simplified to

$$\left\{ \frac{\exp(\epsilon) - \exp(-\tilde{\lambda}_k)}{1 - \exp(-\tilde{\lambda}_k)} \right\}^{Y_k},$$

which must be greater than one, completing the proof.  $\square$